

Calculated and Experimental UV and IR Spectra of Oligo-*para*-phenylenes

Kwangyong Park,^{*} Tae-Won Lee, Min-Ju Yoon, and Jong-In Choe^{†,*}

School of Chemical Engineering and Materials Science,[†] Department of Chemistry, Chung-Ang University, Seoul 156-756, Korea

^{*}E-mail: kypark@cau.ac.kr (K. Park); choeji@cau.ac.kr (J.-I. Choe)

Received August 6, 2013, Accepted November 27, 2013

The quantum mechanical properties of a series of oligo-*para*-phenylenes (**2-11**) were characterized using *DFT* B3LYP/6-311G(d,p) calculations. The global minimum among the various torsional conformers of an oligo-*p*-phenylene is calculated to be a twist conformation. A less stable planar conformation, in which all the dihedral angles in oligo-*p*-phenylene are restricted to be planar, has also been calculated. The total electronic energies, normal vibrational modes, Gibbs free energies, and HOMOs and LUMOs of the two different conformations (twisted and planar) of the oligo-*p*-phenylenes were analyzed. The energy differences between the HOMOs and LUMOs of the substrates are in accord with the maximum absorption peaks of the experimental UV spectra of **2-6**. The calculated normal vibrational modes of **2-6** were comparable with their experimental IR spectra.

Key Words : Oligo-*p*-phenylene, *DFT* B3LYP, HOMO and LUMO, UV, IR

Introduction

Organic π -conjugated compounds have attracted much attention for potential applications in a wide range of optoelectronic devices, such as organic field-effect transistors (OFETs),¹ organic light-emitting diodes (OLEDs),² organic photovoltaic cells,³ and organic solid-state lasers.⁴ Among the variety of π -conjugated compounds, phenylene-based polymers and oligomers are intensively studied due to their excellent chemical and thermal stability. Although initial investigations concentrated on polymeric materials,⁵ their extremely low solubility with increasing chain length has often restricted their application. Accordingly, recent research has tended to take more interest in oligomeric π -conjugated derivatives that are reasonably soluble in common organic solvents, and sublimable under low vacuum pressure conditions.⁶ The facile purification of small oligomers makes such approaches more attractive. Moreover, easy analysis of the exact configuration and conformation of the oligomers allows for precise structure-property correlations to be deduced. A variety of phenylene oligomers with different dimensions and rigidity of the π -backbones have been explored to construct structure-property relationships.⁷

The electronic and optoelectronic properties of the π -conjugated compounds greatly depends on their conjugation lengths. Although phenyl groups connected by a freely rotating bond in polyphenylenes and oligophenylenes may seem to prefer a planar arrangement that maximizes overlaps between adjacent π orbitals, steric hindrance caused by neighboring ortho-substituents twists the phenyls out of the plane.⁸ Because of this, not all phenyl groups in phenylene compounds equally contribute to the conjugation length. This makes the effort to establish the correlation between structure and properties difficult.

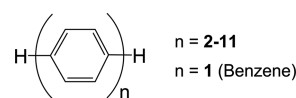
The solid-state morphology of π -conjugated compounds is

one of the most important factors determining the efficiency and stability of electronic and optoelectronic devices. As efficient intermolecular interaction highly enhances the charge carrier mobility, compounds with an appropriate structure to encourage substantial intermolecular π - π overlap are often excellent charge-transporting components.⁹

Conversely, such π - π -stacking tends to form partial crystals that cause electric shortage,¹⁰ and aggregates that cause non-radiative recombination.¹¹ Such processes represent a serious drawback in OLEDs and organic solid-state lasers. It has recently been reported that amorphous materials are often advantageous for OLED applications.¹² Therefore, it is important to understand the spatial conformations and orientations in order to be able to control their properties. The fluorescence and laser properties of D2, C2, and D3 symmetry series oligophenylenes have been reported.¹³ Recently, the torsional potentials and a full-dimensional simulation of the electronic absorption and fluorescence spectra of *para*-phenylene oligomers have been calculated.^{8(a,b)}

This paper reports the molecular structures of oligo-*p*-phenylenes optimized by *DFT* B3LYP/6-311G(d,p). The total electronic energies, normal vibrational modes, Gibbs free energies, HOMO (highest occupied molecular orbital) and LUMO (lowest unoccupied molecular orbital) energies of the phenylene-based oligomers (**2-11**, Scheme 1) were calculated. Also, the calculated gaps between their HOMOs and LUMOs and the λ_{max} values from their experimental UV spectra are compared.

Computational Methods



Scheme 1. The series of oligo-*para*-phenylenes (**2-11**).

The two kinds (twisted and planar) of initial conformations of a series of oligo-*p*-phenylenes (**2-11**) were constructed using molecular mechanics (MM), molecular dynamics (MD), and semi-empirical (AM1) calculations in HyperChem.¹⁴ The twisted structures were found to be the global minimum by rigorous conformational searches using a previously described simulated annealing method.¹⁵ The twisted conformers of **2-11** obtained from the MM/MD and AM1 calculations were fully re-optimized using an *DFT* B3LYP/6-311G(d,p) method in Gaussian 09.^{16(a)} The less stable planar conformations from the restricted flat starting structure were constructed with non-rigorous optimization. The frontier orbitals (HOMO and LUMO) for the oligomers (**2-11**) are drawn by GaussView.^{16(b)}

The B3LYP/6-311G(d,p) method was also used to calculate the normal mode frequencies of the final twisted structures. Each vibrational spectrum shows no negative frequencies, confirming that the optimized structures exist in energy minima. For direct comparison with experimental data, the calculated frequencies were scaled by the recommended scale factor.¹⁷ Furthermore, broadened IR spectra are presented assuming a Lorentzian line width of 10 cm⁻¹.

Experimental Methods

The UV spectra of the oligo-*para*-phenylenes (**2-6**) were collected in a CHCl₃ solution with a JASCO V-670 spectrometer. The Fourier transform IR (FT-IR) spectra were recorded with a Nicolet 6700 FT-IR spectrometer using KBr pellets. Biphenyl and *p*-terphenyl were purchased commercially. *p*-Quarterphenyl was prepared by a literature procedure.¹⁸ *p*-Quinquephenyl and *p*-sexiphenyl were prepared by the following procedures.

Procedure for the Preparation of *p*-Quinquephenyl. 2.0 M aqueous Na₂CO₃ (5.0 mL) was added to a solution of 1,4-dibromobenzene (1.00 g, 4.24 mmol) and Pd(PPh₃)₄ (0.49 g, 0.42 mmol) in toluene (12.0 mL) under Ar atmosphere,

followed by 4-biphenylboronic acid (1.85 g, 9.33 mmol) dissolved in ethanol (8.0 mL). The reaction mixture was heated at reflux for 7 h with vigorous stirring, and diluted with EtOAc (100 mL). The organic layer was washed with 1% aqueous HCl, water, and brine, and then dried over MgSO₄, filtrated through a small pad of silica gel in a sintered glass filter, and concentrated *in vacuo*. The crude compound was washed by methanol to give a white solid in 75% yield: mp 390 °C (lit.¹⁹ 90.45 °C).

Procedure for the Preparation of *p*-Sexiphenyl. 2.0 M aqueous Na₂CO₃ (5.0 mL) was added to a solution of 4,4'-dibromobiphenyl (1.00 g, 3.21 mmol) and Pd(PPh₃)₄ (0.37 g, 0.32 mmol) in toluene (12.0 mL) under Ar atmosphere, followed by 4-biphenylboronic acid (1.40 g, 7.05 mmol) dissolved in ethanol (8.0 mL). The reaction mixture was heated at reflux for 7 h with vigorous stirring and diluted with EtOAc (100 mL). The organic layer was washed with 1% aqueous HCl, water, and brine, and then dried over MgSO₄, filtrated through a small pad of silica gel in a sintered glass filter, and concentrated *in vacuo*. The crude compound was washed by methanol to give a white solid in 69% yield: mp 454 °C (lit.²⁰ 455 °C).

Results and Discussion

The molecular structures of a series of oligo-*p*-phenylenes (**2-11**) were optimized by B3LYP/6-311G(d,p). The total electronic energies, Gibbs free energies, normal vibrational frequencies and the HOMOs (highest occupied molecular orbital) and LUMOs (lowest unoccupied molecular orbital) of ten different oligo-*p*-phenylenes were analyzed.

Table 1 reports the total electronic, HOMO and LUMO energies, and the gaps (excitation energies) between HOMO and LUMO energies of the twisted conformers of the oligo-*p*-phenylenes (**2-11**) calculated by B3LYP/6-311G(d,p). The global minimum among the various torsional conformers of an oligo-*p*-phenylene is calculated to be a twisted confor-

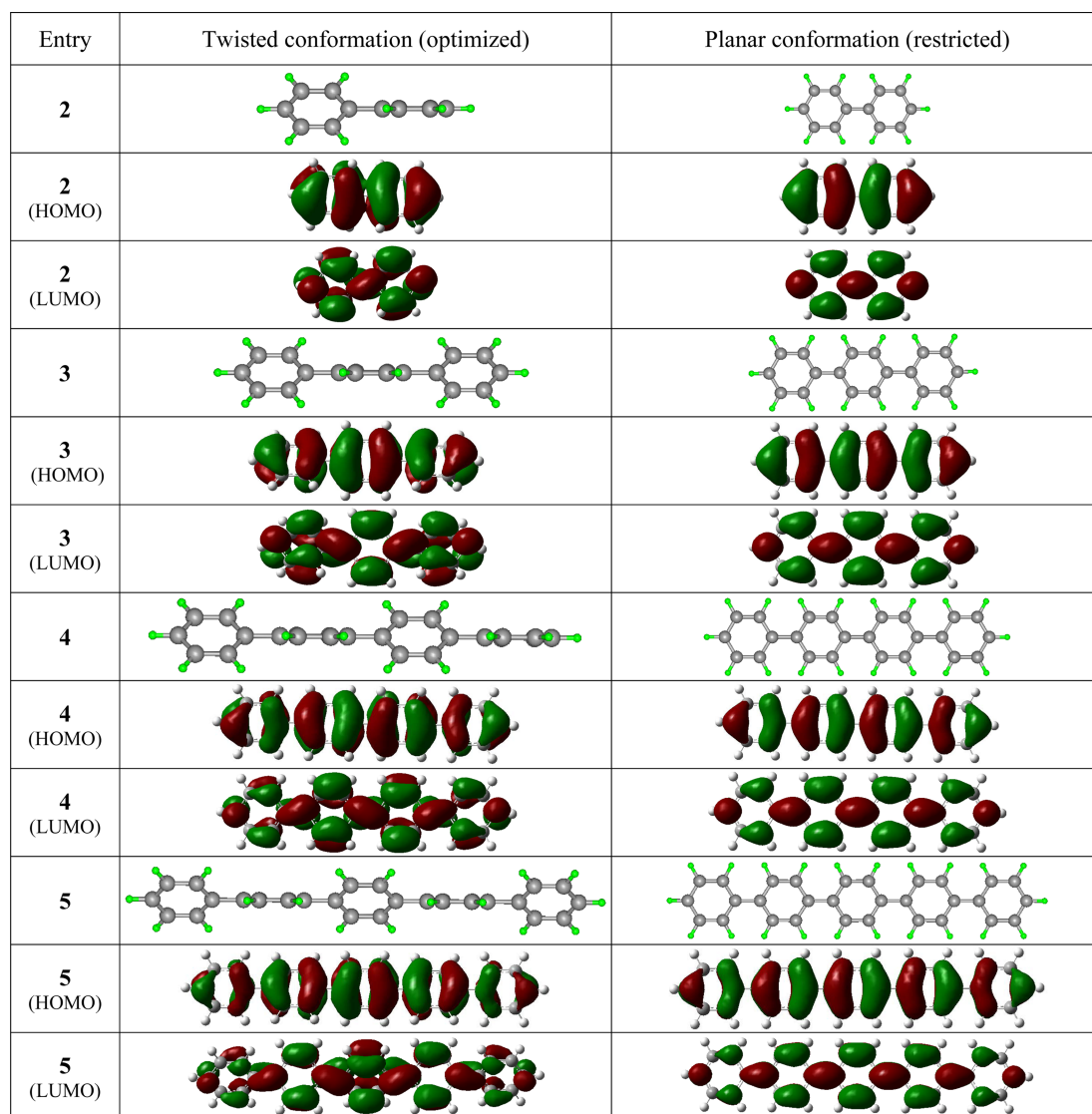
Table 1. B3LYP/6-311G(d,p) calculated total electronic, HOMO and LUMO energies,^a and the comparison of Δ(LUMO-HOMO) energies of the twisted conformers of the oligo-*p*-phenylenes

Energies	Total Electronic	HOMO	LUMO	Δ(LUMO-HOMO)			
				(A.U.)	(A.U.)	(A.U.)	(A.U.)
Unit			Conversion	1.000	627.5096	2625623.8	27.212
Oligo-<i>p</i>-phenylene (Twisted)							
Biphenyl (2)	-463.418	-0.232	-0.036	0.197	123.525	516854.0	5.36
Terphenyl (3)	-694.528	-0.222	-0.047	0.175	109.758	459247.9	4.76
Quaterphenyl (4)	-925.638	-0.217	-0.054	0.164	102.736	429867.1	4.46
Quinquephenyl (5)	-1156.747	-0.214	-0.057	0.157	98.525	412249.2	4.27
Sexiphenyl (6)	-1387.857	-0.213	-0.060	0.153	96.059	401930.5	4.17
Septiphenyl (7)	-1618.967	-0.211	-0.061	0.150	94.114	393791.1	4.08
Octiphenyl (8)	-1850.077	-0.210	-0.062	0.148	92.853	388513.6	4.03
Noniphenyl (9)	-2081.186	-0.209	-0.063	0.146	91.792	384076.2	3.98
Deciphenyl (10)	-2312.296	-0.210	-0.064	0.146	91.434	382579.6	3.97
Undeciphenyl (11)	-2543.406	-0.210	-0.063	0.147	92.313	386255.5	4.00

^aError limits of total electronic energies are 0.00001 Hartree (A.U.).

Table 2. B3LYP/6-311G(d,p) calculated total electronic, HOMO and LUMO energies,^a and the comparison of $\Delta(\text{LUMO-HOMO})$ of the planar conformers of the oligo-*p*-phenylenes

Energies Unit	Total Electronic (A.U.)	HOMO (A.U.)	LUMO (A.U.)	$\Delta(\text{LUMO-HOMO})$			
				(A.U.)	(kcal/mol)	J/mole	eV
Benzene (1)	-232.309	-0.256	-0.009	0.247	155.058	648791.6	6.72
Oligo- <i>p</i> -phenylene (Planar)							
Biphenyl (2)	-463.415	-0.227	-0.045	0.182	114.257	478073.6	4.95
Terphenyl (3)	-694.522	-0.214	-0.059	0.156	97.590	408337.0	4.23
Quaterphenyl (4)	-925.629	-0.208	-0.067	0.142	88.862	371814.6	3.85
Quinquephenyl (5)	-1156.736	-0.205	-0.071	0.133	83.722	350310.7	3.63
Sexiphenyl (6)	-1387.839	-0.202	-0.074	0.128	80.604	337261.4	3.50
Septiphenyl (7)	-1618.950	-0.201	-0.076	0.125	78.370	327914.2	3.40
Octiphenyl (8)	-1850.044	-0.196	-0.078	0.118	74.096	310033.7	3.21
Noniphenyl (9)	-2081.149	-0.195	-0.079	0.116	72.822	304703.6	3.16
Deciphenyl (10)	-2312.271	-0.199	-0.080	0.119	74.561	311976.6	3.23
Undeciphenyl (11)	-2543.379	-0.199	-0.081	0.118	73.996	309613.6	3.21

^aError limits of total electronic energies are 0.00001 Hartree (A.U.).**Figure 1.** The structures of the twisted and planar conformations of oligo-*p*-phenylenes (**2-6**) calculated by B3LYP/6-311G(d,p). The visualization of the optimized structures was performed with PosMol.²² The frontier orbitals (HOMO and LUMO) for the oligomers (**2-11**) are drawn by GaussView.^{16(b)}

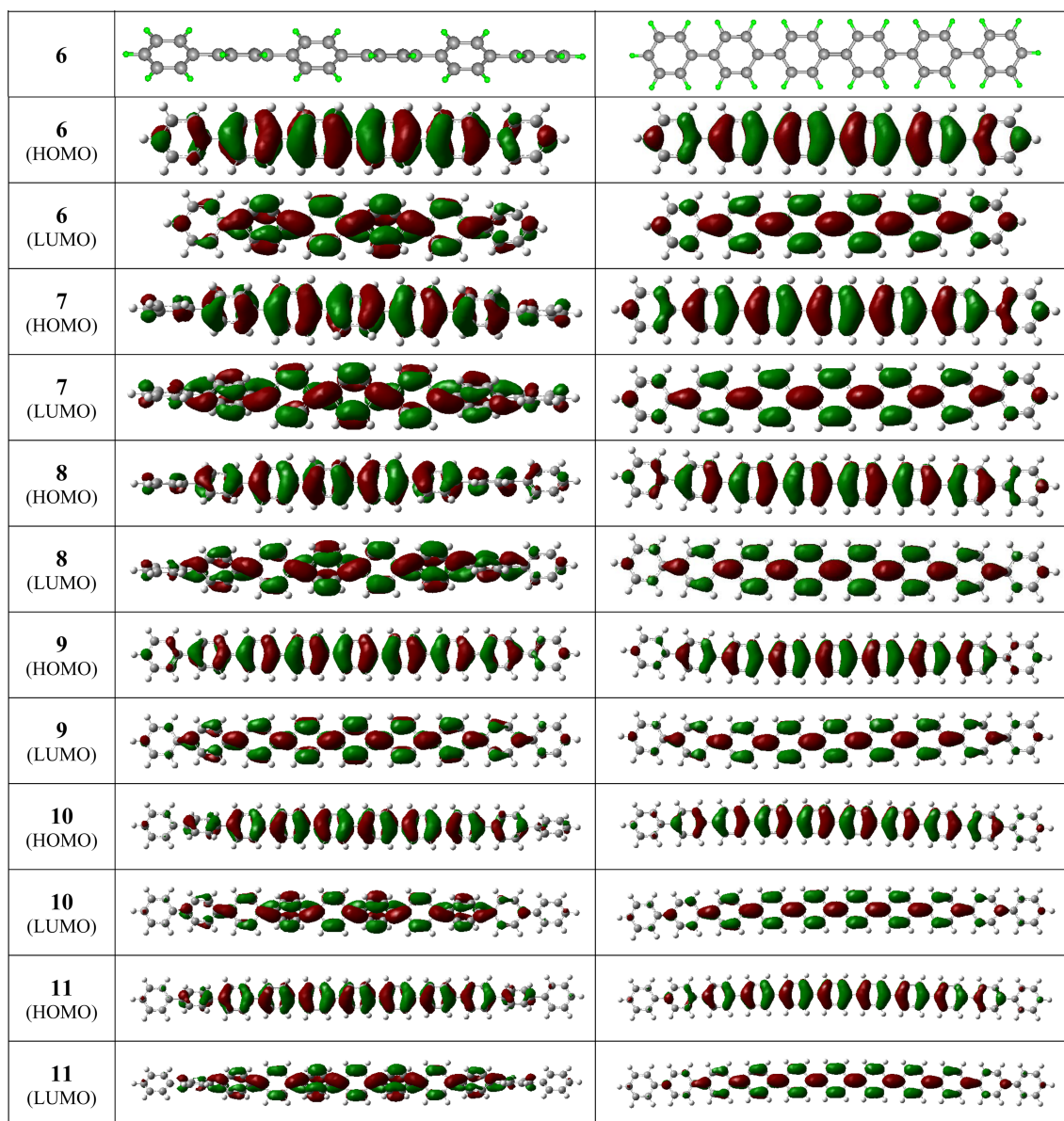


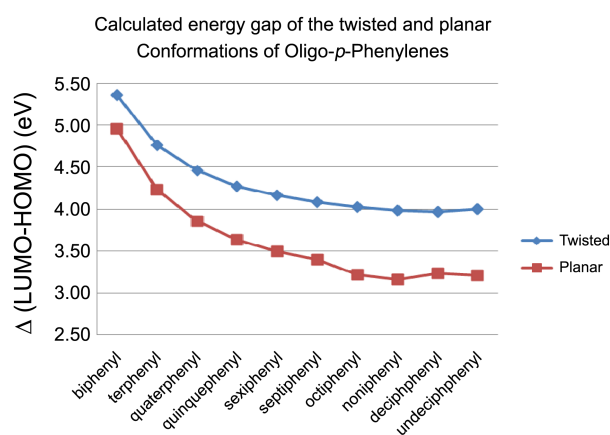
Figure 1. Continued

mation. However, we have also calculated the energies of a less stable planar conformation, in which all the starting dihedral angles in an oligo-*p*-phenylene are restricted to be planar. Table 2 reports the calculated data of the planar conformers of the oligo-*p*-phenylenes. Figure 1 displays the calculated structures of the twisted and planar conformations of oligo-*p*-phenylenes (2-6). The visualization of the optimized structures was performed with PosMol.²¹

Table 3 reports the comparison of $\Delta(\text{LUMO-HOMO})$ energies of the twisted and planar conformations of oligo-*p*-phenylenes calculated by *DFT* B3LYP/6-311G(d,p). Graph 1 displays how the calculated LUMO-HOMO differences decrease with the number of phenyl rings in the series of twisted and planar oligomers (2-11). Phenyl groups connected by a freely rotating bond in oligophenylenes may seem to prefer a planar arrangement maximizing overlaps between adjacent p orbitals. However, steric hindrance twists

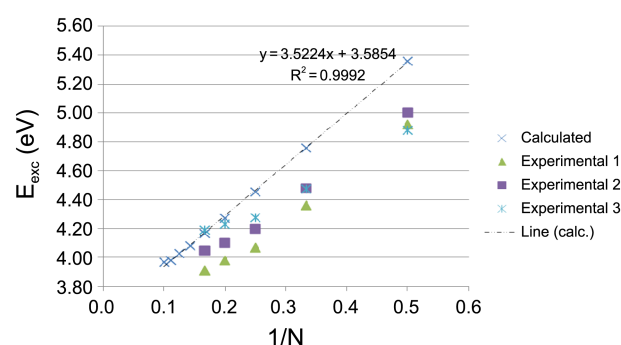
Table 3. Summary of the $\Delta(\text{LUMO-HOMO})$ (eV) of the twisted and planar conformations of oligo-*p*-phenylenes calculated by B3LYP/6-311G(d,p)

Compound	$\Delta(\text{LUMO-HOMO})$	
	Twist	Planar
Benzene (1)	-	6.72
Oligo- <i>p</i> -phenylenes/Conformation		
Biphenyl (2)	5.36	4.95
Terphenyl (3)	4.76	4.23
Quaterphenyl (4)	4.46	3.85
Quinquephenyl (5)	4.27	3.63
Sexiphenyl (6)	4.17	3.50
Septiphenyl (7)	4.08	3.40
Octiphenyl (8)	4.03	3.21
Noniphenyl (9)	3.98	3.16
Deciphenyl (10)	3.97	3.23
Undeciphenyl(11)	4.00	3.21



Graph 1. Dependence of the calculated $\Delta(\text{LUMO-HOMO})$ (eV) on the number of the phenyl rings of the twisted and planar oligo-*p*-phenylenes.

the phenyls out of the planar conformation. The less stable planar conformer has smaller LUMO-HOMO differences than the twisted analogues due to the more effective π -electron delocalization. While the LUMO-HOMO difference exponentially decreases with increasing number of phenyl rings, it remains almost steady after octiphenyl (**8**). This implies that the effective conjugation length and absorption wavelength may not change further after octiphenyl. The conjugation length can be clearly analyzed by the *DFT*



Graph 2. Dependence of the calculated $\Delta(\text{LUMO-HOMO})$ and experimental excitation energies (eV) on the inverse number of the phenyl rings of the twisted oligo-*p*-phenylenes.

calculated frontier orbitals (HOMO and LUMO) of **2-11**, which are drawn in Figure 1. Additional delocalization of π -orbitals after octiphenyl is no longer observed for the HOMOs and LUMOs for the oligomers (**9-11**), which explains the above effective conjugation length very well.

Table 4 reports the dependence of the calculated $\Delta(\text{LUMO-HOMO})$ and experimental excitation energies (eV) on an inverse number of the phenyl rings of the twisted oligo-*p*-phenylenes. Graph 2 shows the dependence of the calculated $\Delta(\text{LUMO-HOMO})$ (eV) on the inverse number of the phenyl rings of the oligo-*p*-phenylenes (**2-6**), which shows that the calculated gaps correlate well with the experimental obser-

Table 4. Dependence of the calculated $\Delta(\text{LUMO-HOMO})$ and experimental excitation energies (eV) on the inverse number of the phenyl rings of the twisted oligo-*p*-phenylenes

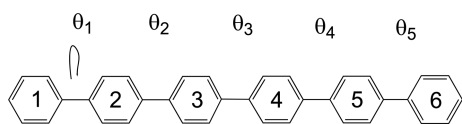
Molecule (N)	Oligo- <i>p</i> -phenylene	1/N	$\Delta(\text{LUMO-HOMO})$ Calculated ^a	Exp. (1) ^b	Exp. (2) ^c	Exp. (3) λ_{max} ^d
2	Biphenyl (2)	0.500	5.36	4.92	5.00	4.88
3	Terphenyl (3)	0.333	4.76	4.36	4.48	4.48
4	Quaterphenyl (4)	0.250	4.46	4.07	4.20	4.28
5	Quinquephenyl (5)	0.200	4.27	3.98	4.10	4.23
6	Sexiphenyl (6)	0.167	4.17	3.91	4.05	4.19

^aError limit is about 0.001 eV. ^{b,c}Experimental excitation energies were already published. ^d λ_{max} (3) represents the maximum absorption wavelength, which is converted to eV (electron volt) unit. These values are obtained from our laboratory.

Table 5. Comparison of the B3LYP/6-311G(d,p) calculated total electronic and Gibbs free energies,^a and torsional angles of the twisted and planar oligo-*p*-phenylenes

Molecule (number)	Compound (conformation)	Total Energy (A.U.)	ΔE^b (kcal)	Gibbs Energy (A.U.)	ΔG^b (kcal)	Torsional Angles (Scheme 2)				
						$\theta(1)$	$\theta(2)$	$\theta(3)$	$\theta(4)$	$\theta(5)$
2	Biphenyl(twisted)	-463.41801	0.00	-463.27174	0.00	40.6				
	Biphenyl(planar)	-463.41457	2.16	-463.26697	3.00	0.0				
3	Terphenyl(twisted)	-694.52771	0.00	-694.30805	0.00	39.2	-39.0			
	Terphenyl(planar)	-694.52162	3.83	-694.29888	5.76	0.0	0.0			
4	Quaterphenyl(twisted)	-925.63755	0.00	-925.34404	0.00	39.2	-37.9	39.2		
	Quaterphenyl(planar)	-925.62871	5.55	-925.33089	8.25					
5	Quinquephenyl(twisted)	-1156.74728	0.00	-1156.38043	0.00	38.9	-37.8	37.8	-38.9	
	Quinquephenyl(planar)	-1156.73559	7.33	-1156.36537	9.45					
6	Sexiphenyl(twisted)	-1387.85711	0.00	-1387.41628	0.00	39.2	-37.9	37.9	-37.9	39.2
	Sexiphenyl(planar)	-1387.83928	11.19	-1387.39317	14.50					

^aError limits of total electronic and Gibbs free energies are 0.00001 Hartree (A.U.). ^bRelative energies (in kcal) between the twisted and planar conformations of the oligo-*p*-phenylenes.



Scheme 2. The notation of torsional angles between adjacent phenyl rings of sexiphenyl (**6**).

variations.^{19,20}

Table 5 reports the total electronic, Gibbs free energies, and torsional angles of oligo-*p*-phenylenes (**2-6**) calculated by B3LYP/6-311G(d,p). The relative energies between the twisted and planar conformations of the oligomers show that the longer planar oligomer gives higher instability by additional steric hindrances between the adjacent phenyl groups of the planar conformer. The torsional angles between adjacent phenyl rings are noted in Scheme 2.

The *DFT* B3LYP/6-311G(d,p) calculated average torsional angles between adjacent phenyl rings of the twisted oligo-*p*-phenylenes (**2-6**) of gas phase in Table 5 are about 39°. Geometry optimization of *para*-biphenyl (**2**) at the Hartree-Fock level (using 6-311++G(d,p) and smaller basis sets) gives a dihedral angle between 46° and 48°. The inclusion of correlation effects at the Møller-Plesset perturbation theory to second-order (MP2) level leads to values between 42° and 46°. The *DFT* calculations of **2** results in smaller dihedral angles (from 39° to 43°). It seems that the best MP2 and *DFT* results are located within the experimental error range obtained for the gas-phase **2** (44.4° (± 1.2°)). While, the experimental torsional angles of the crystal structure of the twisted quarterphenyl (**4**) are about 18°. Generally, in the solid phase, the oligophenyl structures planarize (dihedral angles starting from 2° to 18°). This fact is also reflected in smaller excitation energies in the absorption spectra obtained for films and crystals in comparison with solvent measurements.^{34,35}

The calculated average C-C bond lengths between two phenyl rings in the oligophenylenes are 1.485 (twisted) and 1.489 Å (planar), which are similar to the experimental

average C-C bond lengths (1.499 Å (**4**),²⁹ 1.482 Å (**5**),³³ 1.481 Å (**6**)³³ and 1.479 Å (**7**)³³) of crystal structure. These distances are much shorter than the typical C-C single bond length (1.54 Å) due to the π -electron delocalization of the oligo-*p*-phenylenes.

Table 6 compares the normal vibrational frequencies of the oligo-*p*-phenylenes (**2-6**) calculated by B3LYP/6-311G(d,p) with the intensities of prominent peaks in their experimental IR spectra. Figure 2 show the calculated IR spectra of **2-6**. Most of the frequencies and intensities of the calculated normal modes in the lower frequencies are in accord with the experimental IR peaks. However, some intensities are not in accord, especially the C=C-C bending and C-C stretching normal vibrational modes.

The various peaks from 450 to 900 cm⁻¹ were attributed to the numerous C-H out-of-plane wagging motions of the phenyl rings. The weak peaks around 1000 cm⁻¹ were due to C=C-C bending vibrations. The peaks at about 1400 (weak intensity: antisymmetric CC stretching vibrations) and 1480 cm⁻¹ (variable intensity: symmetric CC stretching vibrations) were due to the different kinds of CC stretching vibrations in the aromatic rings. Particularly, the intensity of the peak at the 1480 cm⁻¹ is becoming stronger as the number of phenyl rings increases, due to the synchronized wagging motions of additional C-H bonds caused by CC stretching vibrations. The weak peaks at about 1600 cm⁻¹ were due to the C-C stretching vibrations between phenyl rings. A series of peaks (3157-3192 cm⁻¹) were attributable to various C-H stretching vibrations.

Conclusions

The total electronic energies, normal vibrational modes, Gibbs free energies, dipole moments, HOMOs, and LUMOs of a series of oligo-*p*-phenylenes (**2-11**) were calculated using B3LYP/6-311G(d,p). The calculated gaps between the HOMOs and LUMOs are in excellent agreement with the maximum absorption peaks in experimental UV spectra. The less stable planar conformer has smaller LUMO-HOMO

Table 6. Main features of B3LYP/6-311G(d,p) calculated normal vibrational modes and experimental IR peaks of the twisted oligo-*p*-phenylenes (**2-6**)

Oligo- <i>p</i> -phenylene Normal Mode	Biphenyl (2)		Terphenyl (3)		Quaterphenyl (4)		Quinquephenyl (5)		Sexiphenyl (6)	
	Exp. ^a	Calc. ^b	Exp.	Calc.	Exp.	Calc.	Exp.	Calc.	Exp.	Calc.
C-H out-of-planar wagging	610(w)	626.5	461(w)	497.6	462(w)	504.1	458(w)	501.8	458(w)	504.0
	698(s)	716.5	689(s)	697.2	688(s)	698.1	689(s)	698.0	689(s)	698.3
	728(s)	756.6	745(s)	752.0	753(s)	758.6	754(s)	763.2	746(s)	764.7
	903(w)	923.4	838(m)	842.3	826(s)	830.4	826(s)	822.9	838(m)	818.4
C=C-C bendings		1002.6	1003(w)	998.8	1001(w)	997.2	1001(w)	996.3	1003(w)	996.0
C=C stretchings	1344(m)	1428.9	1404(w)	1397.5	1400(w)	1394.3	1400(w)	1392.2	1404(w)	1391.9
	1481(s)	1481.4	1480(m)	1481.8	1481(m)	1482.9	1480(s)	1482.9	1480(m)	1483.1
C-C stretchings	1569(w)	1646.1		1606.4		1605.9		1606.1		1605.0
C-H stretchings	3033(m)	3157	3033(m)	3158	3033(m)	3159	3032(m)	3163	3033(m)	3158
		~3192		~3193		~3194		~3190		~3193

^aExperimental infrared peak. Intensity: (s) = strong, (m) = medium, (w) = weak. ^bThe calculated vibrational frequency is scaled by multiplication by 0.977, adjusted it for favorable to comparison with experimental observations of lower frequencies.¹⁸

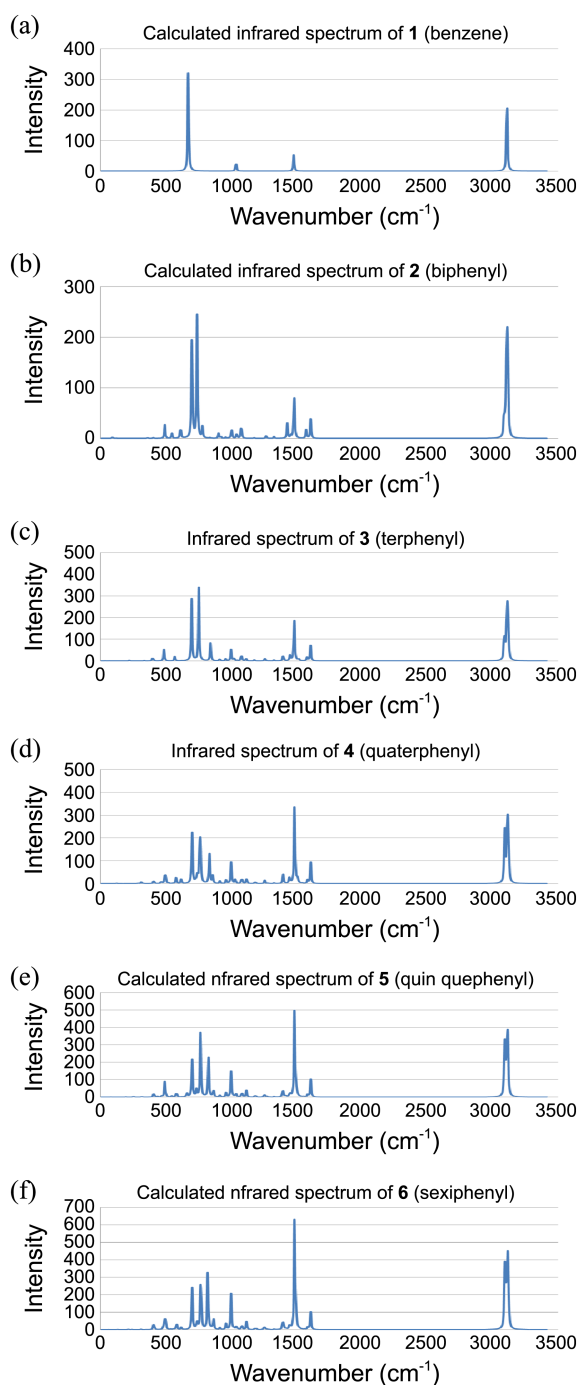


Figure 2. The infrared spectra of the twisted conformations of oligo-*p*-phenylenes (**1-6**) calculated by B3LYP/6-311G(d,p).

differences than the twisted analogues due to more effective π -electron delocalization. Most of the frequencies and intensities of the calculated normal modes of **2-6** favorably agree with the experimental IR peaks. Particularly, the intensity of the peak at the 1480 cm^{-1} is becoming stronger as the number of phenyl rings increases, due to the synchronized wagging motions of additional C-H bonds caused by CC stretching vibrations.

Acknowledgments. This work was supported by the

Chung-Ang University Excellent Student Scholarship and the National Research Foundation of Korea Grant funded by the Korean Government (MEST) (grant No. NRF-2012-R1A1A2043846).

References

- (a) Yamamoto, T.; Nishimura, T.; Mori, T.; Miyazaki, E.; Osaka, I.; Takimiya, K. *Org. Lett.* **2012**, *14*, 4914. (b) Madathil, P. K.; Lim, J. G.; Kim, T. D.; Beckmann, D.; Mavrinskiy, A.; Pisula, W.; Baumgarten, M.; Müllen, K.; Lee, K. S. *J. Nanosci. Nanotechnol.* **2012**, *12*, 4269. (c) Katsuta, S.; Miyagi, D.; Yamada, H.; Okujima, T.; Mori, S.; Nakayama, K.; Uno, H. *Org. Lett.* **2011**, *13*, 1454. (d) Yasuda, T.; Saito, M.; Nakamura, H.; Tsutsui, T. *Chem. Phys. Lett.* **2008**, *452*, 110.
- (a) Lee, C. W.; Kim, J. K.; Joo, S. H.; Lee, J. Y. *ACS Appl. Mater. Inter.* **2013**, *5*, 2169. (b) Li, Z.; Jiao, B.; Wu, Z.; Liu, P.; Ma, L.; Lei, X.; Wang, D.; Zhou, G.; Hu, H.; Hou, X. *J. Mater. Chem.* **2013**, *1*, 2183. (c) Sasabe, H.; Kido, J. *J. Mater. Chem.* **2013**, *1*, 1699. (d) Fu, H.; Cheng, Y.; Chou, P.; Chi, Y. *Mater. Today* **2011**, *14*, 472. (e) Zhu, X.; Peng, J.; Cao, Y.; Roncali, J. *Chem. Soc. Rev.* **2011**, *40*, 3509. (f) Sasabe, H.; Kido, J. *Chem. Mater.* **2011**, *23*, 621.
- (a) Gong, J.; Liang, J.; Sumathy, K. *Renew. Sust. Energ. Rev.* **2012**, *16*, 5848. (b) Kumar, P.; Chand, S. *Prog. Photovolt: Res. Appl. Mater. Express* **2012**, *2*, 814. (c) Li, C.; Liu, M.; Pschirer, N. G.; Baumgarten, M.; Müllen, K. *Chem. Rev.* **2010**, *110*, 6817.
- (a) Chénais, S.; Forget, S. *Polym. Int.* **2012**, *61*, 390. (b) Schneider, D.; Rabe, T.; Riedl, T.; Dobbertin, T.; Kröger, M.; Becker, E.; Johannes, H. H.; Kowalsky, W.; Weimann, T.; Wang, J.; Hinze, P. *J. Appl. Phys.* **2005**, *98*, 043104. (c) Kranzelbinder, G.; Leising, G. *Rep. Prog. Phys.* **2000**, *63*, 729.
- (a) Schmaltz, B.; Weil, T.; Müllen, K. *Adv. Mater.* **2009**, *21*, 1067. (b) Grimsdale, A. C.; Müllen, K. *Macromol. Rapid Comm.* **2007**, *28*, 1676.
- (a) Türp, D.; Nguyen, T.; Baumgarten, M.; Müllen, K. *New J. Chem.* **2012**, *36*, 282. (b) Iyoda, M. *Adv. Synth. Catal.* **2009**, *351*, 984.
- (a) Nehls, B. S.; Galbrecht, F.; Bilge, A.; Brauer, D. J.; Lehmann, C. W.; Scherf, U.; Farrell, T. *Org. Biomol. Chem.* **2005**, *3*, 3213. (b) Mabbs, R.; Nijegorodov, N.; Downey, W. S. *Spectrochim. Acta A* **2003**, *59*, 1329. (c) Nijegorodov, N. I.; Downey, W. S.; Danailov, M. B. *Spectrochim. Acta A* **2000**, *56*, 783.
- (a) Lukeš, V.; Šolc, R.; Barbatti, M.; Elstner, M.; Lischka, H.; Kauffmann, H. *J. Chem. Phys.* **2008**, *129*, 164905. (b) Lukeš, V.; Aquino, A.; Lischka, H.; Kauffmann, H. *J. Phys. Chem. B* **2007**, *111*, 7954. (c) Baker, K. N.; Fratini, A. V.; Resch, T.; Knachel, H. C.; Adams, W. W.; Soccia, E. P.; Farmer, B. L. *Polymer* **1993**, *34*, 1571.
- Kjelstrup-Hansen, J.; Norton, J. E.; Silva Filho, D. A.; Bredas, J. L.; Rubahn, H. G. *Org. Electron.* **2009**, *10*, 1228.
- (a) Joswick, M. D.; Campbella, I. H.; Barashkov, N. N.; Ferraris, J. P. *J. Appl. Phys.* **1996**, *80*, 2883. (b) Kuwabara, Y.; Ogawa, H.; Inada, H.; Noma, N.; Shirota, Y. *Adv. Mat.* **1994**, *6*, 677.
- Shirota, Y. *J. Mater. Chem.* **2005**, *15*, 75.
- (a) Lyu, Y. Y.; Kwak, J. H.; Kwon, O. H.; Lee, S. H.; Kim, D. Y.; Lee, C. H.; Cha, K. H. *Adv. Mater.* **2008**, *20*, 2720. (b) Li, J.; Ma, C.; Tang, J.; Lee, C. S.; Lee, S. *Chem. Mater.* **2005**, *17*, 615.
- Mabbs, R.; Nijegorodov, N.; Downey, W. S. *Spectrochimica Acta Part A* **2003**, *59*, 1329.
- HyperChem Release 7.5*, Hypercube, Inc.: Waterloo, Ontario, Canada, 2002.
- Choe, J.-I.; Kim, K.; Chang, S.-K. *Bull. Korean Chem. Soc.* **2000**, *21*, 465.
- (a) Frisch, M. J.; Trucks, G. W.; Schlegel, H. B.; Scuseria, G. E.; Robb, M. A.; Cheeseman, J. R.; Scalmani, G.; Barone, V.; Mennucci,

- B.; Petersson, G. A.; Nakatsuji, H.; Caricato, M.; Li, X.; Hratchian, H. P.; Izmaylov, A. F.; Bloino, J.; Zheng, G.; Sonnenberg, J. L.; Hada, M.; Ehara, M.; Toyota, K.; Fukuda, R.; Hasegawa, J.; Ishida, M.; Nakajima, T.; Honda, Y.; Kitao, O.; Nakai, H.; Vreven, T.; Montgomery, Jr., J. A.; Peralta, J. E.; Ogliaro, F.; Bearpark, M.; Heyd, J. J.; Brothers, E.; Kudin, K. N.; Staroverov, V. N.; Kobayashi, R.; Normand, J.; Raghavachari, K.; Rendell, A.; Burant, J. C.; Iyengar, S. S.; Tomasi, J.; Cossi, M.; Rega, N.; Millam, J. M.; Klene, M.; Knox, J. E.; Cross, J. B.; Bakken, V.; Adamo, C.; Jaramillo, J.; Gomperts, R.; Stratmann, R. E.; Yazyev, O.; Austin, A. J.; Cammi, R.; Pomelli, C.; Ochterski, J. W.; Martin, R. L.; Morokuma, K.; Zakrzewski, V. G.; Voth, G. A.; Salvador, P.; Dannenberg, J. J.; Dapprich, S.; Daniels, A. D.; Farkas, Ö.; Foresman, J. B.; Ortiz, J. V.; Cioslowski, J.; Fox, D. J. *Gaussian 09*, Revision C.01, Gaussian, Inc., Wallingford CT, 2009. (b) GaussView, Version 5, Dennington, Roy; Keith, Todd; Millam, John. Semichem Inc., Shawnee Mission, KS, 2009.
17. *Exploring Chemistry with Electronic Structure Methods*, 2nd ed.; Foresman, J. B., Frisch, A., Eds.; Gaussian Inc.: Pittsburgh, PA, 1996. Page 63: Raw normal vibrational frequency values computed at the Hartree-Fock level contain known systematic errors due to the neglect of electron correlation, resulting in overestimates.
18. Jo, H.; Kim, C.-B.; Ryoo, T.-Y.; Ahn, B.-K.; Park, K. *Bull. Korean Chem. Soc.* **2010**, *31*, 3749.
19. Davis, M. C.; Groshens, T. J. *Synthetic Communications* **2011**, *41*, 206.
20. Ozasa, S.; Fujioka, Y.; Ibuki, E. *Chem. Pharm. Bull.* **1982**, *30*, 2698.
21. Lee, S. J.; Chung, H. Y.; Kim, K. S. *Bull. Korean Chem. Soc.* **2004**, *25*, 1061.
22. Grein, F. *J. Mol. Struct. THEOCHEM* **2003**, *624*, 23.
23. Karpfen, A.; Choi, C. H.; Kertesa, M. *J. Phys. Chem. A* **1997**, *101*, 7426.
24. Tsuzuki, S.; Uchimaru, T.; Matsumura, M.; Mikami, M.; Tanabe, K. *J. Chem. Phys.* **1999**, *110*, 2858.
25. Arulmozhiraja, A.; Fujii, T. *J. Chem. Phys.* **2001**, *115*, 10589.
26. Fabiano, E.; Della Sala, F. *Chem. Phys. Lett.* **2006**, *418*, 496.
27. Rubio, M.; Merchan, M.; Orti, E.; Roos, B. O. *Chem. Phys. Lett.* **1995**, *234*, 373.
28. Almenningen, A.; Bastiansen, O.; Fernholt, L.; Cyvin, B. N.; Cyvin, S. J.; Samdal, S. *J. Mol. Struct. (Theochem)* **1985**, *128*, 59.
29. Baudour, J.-L.; Délugeard, Y.; Rivet, P. *Acta Cryst.* **1978**, *B34*, 625.
30. Charbonneau, G. P.; Delugeard, Y. *Acta Crystallogr., Sect. B* **1976**, *32*, 1420.
31. Baudour, J. L.; Toupet, L.; Delugeard, Y.; Ghemid, S. *J. Acta Crystallogr., Sect. C* **1986**, *42*, 1211.
32. Delugeard, Y. *Acta Crystallogr., Sect. B* **1976**, *32*, 702.
33. Baker, K. N.; Fratini, A. V.; Resch, T.; Knachel, H. C.; Adams, W. W.; Soggi, E. P.; Farmer, B. L. *Polymer* **1993**, *34*, 1571.
34. Matsuoka, S.; Fujii, H.; Yamada, T.; Pac, C.; Ishida, A. *J. Phys. Chem.* **1991**, *95*, 5802.
35. Mabbs, R.; Nijegorodov, N.; Downey, W. S. *Spectrochim. Acta, Part A* **2003**, *59*, 1329.
-